

To appear in *The Astrophysical Journal Letters*, the 2003-November-20th issue

Modeling the Infrared Emission from the ϵ Eridani Disk

Aigen Li, J.I. Lunine, and G.J. Bendo

*Theoretical Astrophysics Program, Steward Observatory and Lunar and Planetary Laboratory,
University of Arizona, Tucson, AZ 85721;
agli@lpl.arizona.edu, jlunine@lpl.arizona.edu, gbendo@as.arizona.edu*

ABSTRACT

We model the infrared (IR) emission from the ring-like dust disk around the main-sequence (MS) star ϵ Eridani, a young analog to our solar system, in terms of a porous dust model previously developed for the extended wedge-shaped disk around the MS star β Pictoris and the sharply truncated ring-like disks around the Herbig Ae/Be stars HR 4796A and HD 141569A. It is shown that the porous dust model with a porosity of $\sim 90\%$ is also successful in reproducing the IR to submillimeter dust emission spectral energy distribution as well as the $850\ \mu\text{m}$ flux radial profile of the dust ring around the more evolved MS star ϵ Eri. Predictions are made for future *SIRTF* observations which may allow a direct test of the porous dust model.

Subject headings: circumstellar matter — dust, extinction — infrared: stars — planetary systems: protoplanetary disks — stars: individual (ϵ Eridani)

1. Introduction

Together with Vega, Fomalhaut (α PsA), and β Pictoris, the nearby (distance to the Earth $d \approx 3.2\ \text{pc}$) low-mass ($m_\star \approx 0.8m_\odot$) K2V main-sequence (MS) star ϵ Eridani constitutes the “Big-Four” family of prototypical “Vega-excess” stars, which are MS stars with infrared (IR) radiation in excess of what is expected from their stellar photospheres (Gillett 1986). The IR excess associated with “Vega-excess” stars is generally attributed to the thermal emission of dust grains orbiting the central star in the form of a disk or ring and heated by its stellar radiation. The dust is thought to be “second generational” in nature rather than “primordial”; i.e., the dust is considered as *debris* generated by collisions of larger objects such as cometary and/or asteroidal bodies rather than *remnants* left over from the star formation process (Backman & Paresce 1993; Lagrange, Backman, & Artymowicz 2000; Zuckerman 2001).

In recent years, ϵ Eri has received much attention since it is thought to be analogous to the solar system at an age about 10–20% of that of the Sun: (1) in comparison with the other three “Big-Four” prototypes which all are much more luminous A-type stars, ϵ Eri is *closer* in type, mass,

and luminosity ($L_{\star} \approx 0.33L_{\odot}$; Soderblom & Däppen 1989) to the Sun (see Greaves & Holland 2000); (2) ϵ Eri has a ring-like structure of ~ 55 AU in radius (which is very similar to the Kuiper Belt in size) and a central cavity inside ~ 30 AU (which is equivalent in scale to Neptune’s orbit) as revealed by its $850 \mu\text{m}$ image obtained using the SCUBA (*Submillimetre Common-User Bolometer Array*) camera at the *James Clerk Maxwell Telescope* (JCMT; Greaves et al. 1998). (3) as the oldest (with an age of ≈ 800 Myr; Henry et al. 1996) “Big-Four” Vega-type star, the formation of planets in its disk may have completed since planet formation is thought to be complete by about 10 to 100 Myr (Lissauer 1993); (4) a roughly Jupiter-mass planet with a period of ~ 6.9 yr appears to be present inside the central cleared region of the ϵ Eri disk, as suggested by the radial velocity measurements spanning the years 1980.8–2000.0 (Hatzes et al. 2000).

To better understand the origin and evolution of protoplanetary dust disks and the formation process of planetary systems, we need to know the physical, chemical, and dynamical properties of their constituent grains. In previous papers (Li & Greenberg 1998, Li & Lunine 2003a,b), we have shown that a simple porous dust model is successful in reproducing the spectral energy distributions from the near-IR to millimeter wavelengths of the disks around the Herbig Ae/Be stars HR 4796A and HD 141569A and the Vega-type star β Pictoris, including the $9.7 \mu\text{m}$ amorphous and the $11.3 \mu\text{m}$ crystalline silicate features or the $7.7 \mu\text{m}$ and $11.3 \mu\text{m}$ polycyclic aromatic hydrocarbon (PAH) features. In this *Letter* we will study the dust IR to submillimeter emission of the disk around the more evolved star ϵ Eri. The objectives of this *Letter* are four-fold: (1) we wish to infer the physical and chemical properties of the dust in the ϵ Eri disk and to infer the disk structure; (2) we wish to gain insights into the evolution of dust mass, size, morphology, and mineralogy at different stellar ages; (3) we wish to know how widely applicable is the porous dust model; if it can be shown that the porous dust model is “universally” valid for disks at different evolutionary stages and with different geometrical structures, it will be a valuable guide for interpreting future data sets obtained by the upcoming *Space Infrared Telescope Facility* (SIRTF); (4) we wish to make mid-IR spectral, imaging and broadband photometry predictions for the ϵ Eri disk; these predictions can be compared to future SIRTF observations in order to test further the validity of the porous dust model.

2. The Porous Dust Model

We have discussed in detail in Li & Greenberg (1998) and Li & Lunine (2003a,b) that the dust in protoplanetary disks most likely consists of porous aggregates of protostellar materials of interstellar origin, although there is no consensus regarding the degree to which the original interstellar materials have been processed in protostellar nebulae. Unless there are IR signatures (e.g. the $11.3 \mu\text{m}$ crystalline silicate feature) suggestive of the thermal history of the dust available, it is difficult to determine the composition of the dust a priori. Therefore, in modeling the IR emission of dust disks we usually invoke two extreme dust types: “*cold-coagulation*” dust made of coagulated but otherwise unaltered protostellar interstellar grains, and “*hot-nebula*” dust made of

grains that are highly-processed in protostellar nebulae where silicate dust is annealed and carbon dust is destroyed by oxidization (see Li & Lunine 2003a,b for details). Since the ϵ Eri disk is too cold to emit at the mineralogical “fingerprinting” mid-IR features (e.g. the 9.7 and 11.3 μm silicate bands and the 3.3, 6.2, 7.7, 8.6, and 11.3 μm PAH bands), we will just adopt the “cold-coagulation” dust model. It has been shown in Li & Lunine (2003a,b) that the major differences between the IR emission from these two dust models lie in their mid-IR spectral features, while their continuum emission are very similar.

For the dust properties, we take the porosity (or fluffiness; the fractional volume of vacuum in a grain) to be $P = 0.90$ for 3 reasons: (i) dust models with $P \simeq 0.90$ are successful in modeling the IR emission from the disks around HR 4796A (Li & Lunine 2003a), HD 141569A (Li & Lunine 2003b), and β Pictoris (Li & Greenberg 1998); (ii) a porosity in the range of $0.80 \lesssim P \lesssim 0.90$ is expected for dust aggregates formed through coagulation as demonstrated both theoretically (Cameron & Schneck 1965) and experimentally (Blum, Schräpler, & Kozasa 2003); (iii) a porosity of $P \simeq 0.90$ for the “cold-coagulation” dust is consistent with the mean mass density of cometary nuclei for which the ice-coated “cold-coagulation” dust aggregates are plausible building blocks (see Greenberg & Li 1999). We assume a power-law dust size distribution $dn(a)/da \propto a^{-\alpha}$ which is characterized by a lower-cutoff a_{min} , upper-cutoff a_{max} and power-law index α ; we take $a_{\text{min}} = 1 \mu\text{m}$ and $a_{\text{max}} = 1 \text{ cm}$ (see Li & Lunine 2003a,b).¹ As far as the dust composition is concerned, we take the “cold-coagulation” dust model – the dust is assumed to be composed of amorphous silicate and carbonaceous materials (and H₂O-dominated ices in regions colder than ~ 110 – 120 K); the mixing mass ratios for the silicate, carbon and ice constituent grains are approximately derived in Li & Lunine (2003a), by assuming cosmic abundance, to be $m_{\text{carb}}/m_{\text{sil}} \approx 0.7$ and $m_{\text{ice}}/(m_{\text{sil}} + m_{\text{carb}}) \approx 0.8$ where m_{sil} , m_{carb} , and m_{ice} are respectively the total mass of the silicate, carbon, and ice subgrains.

Guided by the 850 μm SCUBA/JCMT image and the 850 μm flux radial profile (see Figs. 1,2 of Greaves et al. 1998), we will adopt a Gaussian functional formula for the dust spatial surface density distribution $\sigma(r) = \sigma_p \exp[-4 \ln 2 \{(r - r_p)/\Delta\}^2]$ which describes the dust ring peaking at ~ 55 AU from the star. The extent of the ϵ Eri disk is cut off at an inner boundary of $r_{\text{in}} = 0.05$ AU where small grains are heated to temperatures $\gtrsim 1500$ K, and an outer boundary of $r_{\text{out}} = 200$ AU outside of which there is little dust emission.

We use Mie theory together with the Bruggman effective medium theory (Krügel 2003) to calculate the absorption cross sections of the fluffy heterogeneous dust aggregates. Dielectric functions are taken from Draine & Lee (1984) for amorphous silicate dust; Li & Greenberg (1997) for carbonaceous dust; and Li & Greenberg (1998) for H₂O-dominated “dirty” ice. The ϵ Eri stellar radiation is approximated by the Kurucz (1979) model atmosphere spectrum for K2V stars with

¹We assume all grains are spherical in shape; the grain size a is defined as the radius of the sphere encompassing the entire aggregate. The choice of a_{min} and a_{max} , as extensively discussed in Li & Lunine (2003a,b) for the disks around HR 4796A and HD 141569A, will not affect our conclusion.

an effective temperature of $T_{\text{eff}} = 5000$ K, a surface gravity of $\lg g=4.0$, and a solar metallicity $Z/Z_{\odot} = 1$. The calculated dust IR emission spectrum is compared with the IRAS flux at 12, 25, 60, and 100 μm and the SCUBA flux at 450 and 850 μm (see Table 1 in Greaves et al. 1998). There also exist 1300 μm photometric measurements for the ϵ Eri disk (e.g., Chini, Krügel, & Kreysa 1990, Chini et al. 1991), but we will not include these data since these measurements were all made using single-element bolometers with telescope beams smaller than the disk extent so that the flux obtained by these measurements may be underestimated (Zuckerman & Becklin 1993, Weintraub & Stein 1994).

3. Model Results

The model has four free parameters: α – the dust size distribution power-law exponent, r_p – the disk radial location where the dust spatial distribution peaks; Δ – the FWHM of the dust spatial distribution; σ_p – the mid-plane surface density at $r = r_p$. Observational constraints include the observed IR spectral energy distribution and the SCUBA 850 μm image. The latter is particularly important for constraining the spatial distribution of the dust in the ϵ Eri disk. Instead of using the smoothed 850 μm image presented in Greaves et al. (1998), we constructed an unsmoothed 850 μm image from all 1997–2000 data in the SCUBA archive using the data reduction procedure outlined in Bendo et al. (2003). However, both the image and the radial profile obtained from our analysis show an overall good agreement with those of Greaves et al. (1998).

As shown in Figure 1, the $P = 0.90$ porous dust model² with $\alpha \approx 3.1$, $r_p \approx 55$ AU, $\Delta \approx 30$ AU, and $\sigma_p \approx 966 \text{ cm}^{-2}$ provides an almost perfect fit to the observed IR to submillimeter emission (Fig. 1a) and to the azimuthally averaged flux radial distribution at 850 μm (Fig. 1b) except that the model is deficient in emitting at 850 μm inside ~ 28 AU (see below for further discussion).³ This model requires a total dust mass of $m_d \approx 4.22 \times 10^{25} \text{ g} \approx 7.1 \times 10^{-3} m_{\oplus}$. Let the goodness of fit be $\chi^2/N_{\text{obs}} \equiv \frac{1}{N_{\text{obs}}} \sum_{i=1}^{N_{\text{obs}}} \{([\lambda F_{\lambda}]_{\text{mod}} - [\lambda F_{\lambda}]_{\text{obs}}) / [\lambda \Delta F_{\lambda}]_{\text{obs}}\}^2$ where $[\lambda F_{\lambda}]_{\text{obs}}$ and $[\lambda F_{\lambda}]_{\text{mod}}$ are respectively the observed and model-predicted flux densities, $[\lambda \Delta F_{\lambda}]_{\text{obs}}$ is the observational flux uncertainty, $N_{\text{obs}} \equiv 6$ is the number of data points to be fit. This model gives $\chi^2/N_{\text{obs}} \approx 0.54$.

The apparent rise in flux density within $r \approx 4.5''$ (~ 15 AU) was also seen in the smoothed SCUBA 850 μm radial profile of Greaves et al. (1998; see their Fig. 2). This rise may be associated with the “*small peak 5''–10'' south of star*” seen in the SCUBA 850 μm image (see Fig. 1 of Greaves et al. 1998). If this is real, we then need to resort to an additional dust component lying close to the star. This inner warm component would resemble the zodiacal dust cloud in our solar system.

²In fact the porosity is reduced to $P' \approx 0.73$ after ices fill in some of the vacuum (see Appendix B in Li & Lunine 2003a) which occurs at $r \gtrsim 3$ AU.

³The model-predicted 850 μm radial profile is convolved with the SCUBA 14'' beam using the actual SCUBA point spread function (PSF).

However, the SCUBA images are quite noisy in the inner region, so the anomalous emission inside $r \approx 4.5''$ may be instrumental noise or image processing artifacts. We therefore exclude this “inner component” emission in our model.

4. Discussion

We have seen in §3 that the very same porous dust model shown to be successful in modeling the IR emission from the dust disks around the Herbig Ae/Be stars HR 4796A (Li & Lunine 2003a) and HD 141569A (Li & Lunine 2003b) and the young MS star β Pictoris (Li & Greenberg 1998) is also successful in reproducing the IR to submillimeter SED as well as the $850\ \mu\text{m}$ flux density radial profile of the more evolved MS star ϵ Eri (~ 800 Myr old), although the model appears unable to provide sufficient $850\ \mu\text{m}$ emission inside ~ 28 AU (see Fig. 1b). It is very likely that this inner component emission is not real (see §3); but if one really wants to push us to account for this emission, we find that it could be explained by invoking an inner “zodiacal” dust cloud of $\sim 5.2 \times 10^{-4} m_{\oplus}$ mass located at ~ 2 AU from the star.

SIRTF will be capable of sensitive imaging using the *Infrared Array Camera* (IRAC) at 3.6, 4.5, 5.8, and $8.0\ \mu\text{m}$, and using the *Multiband Imaging Photometer* (MIPS) at 24, 70, and $160\ \mu\text{m}$. SIRTF will also be able to perform low-resolution 5– $40\ \mu\text{m}$ and high-resolution 10– $37\ \mu\text{m}$ spectroscopic observations using the *Infrared Spectrograph* (IRS) instrument. However, the dust in the ϵ Eri disk seems to be too cold to emit in an appreciable quantity in the IRAC bands (see Fig. 1a). Neither can this dust be heated sufficiently to emit at the characteristic mid-IR spectral features. But the MIPS imaging will provide powerful constraints on the ϵ Eri dust spatial distribution. We have therefore calculated the MIPS 24, 70, and $160\ \mu\text{m}$ flux density radial distributions for the best-fit porous dust model (see Fig. 1c). All profiles are convolved with the MIPS model PSFs. In Table 1 we show the model-predicted band-averaged intensities.

Table 1: Dust IR emission (Jy) integrated over SIRTF bands predicted for the porous dust model. Also tabulated are the stellar photospheric emission (Jy).

Instrument	IRAC	IRAC	IRAC	IRAC	MIPS	MIPS	MIPS
λ_{eff}	$3.6\ \mu\text{m}$	$4.5\ \mu\text{m}$	$5.8\ \mu\text{m}$	$8\ \mu\text{m}$	$24\ \mu\text{m}$	$70\ \mu\text{m}$	$160\ \mu\text{m}$
dust	1.35×10^{-5}	2.03×10^{-5}	3.43×10^{-5}	8.47×10^{-5}	0.10	1.55	1.71
stellar	65.4	40.7	28.6	16.4	2.26	0.25	0.056

The dust in the ϵ Eri disk is stable against the radiation pressure. As shown in Figure 2a, β_{RP} , the ratio of radiative pressure (RP) force to gravitational force is found to be smaller than 0.3 for all grains. But the Poynting-Robertson (PR) drag would remove grains smaller than $\sim 270\ \mu\text{m}$

at $r = 55$ AU in a timescale (τ_{PR}) shorter than the age of the ϵ Eri system (see Fig. 2b).⁴ By integrating the PR dust removal rate $(4\pi/3) \rho a^3 / \tau_{\text{PR}}(a, r)$ [where ρ is the mass density of the dust aggregate: $\rho \approx 0.25$ (0.46) g cm^{-3} for the $P = 0.90$ ($P' = 0.73$ ice-coated) cold-coagulation type dust; see Appendix B in Li & Lunine 2003a] over the whole size range and over the entire disk, we estimate the PR dust mass loss rate to be $\approx 4.3 \times 10^{-11} m_{\oplus} \text{yr}^{-1}$ for the porous dust model. Over the life span of ϵ Eri, roughly $0.034 m_{\oplus}$ of dust is lost by the PR drag. Therefore, the observed grains need to be continuously replenished, very likely from cascade collisions and evaporation of larger bodies such as comets and/or asteroids.

The inner “zodiacal” cloud, *if it indeed exists*, could be maintained by grains released from the sublimation of bombarding comets near the star.⁵ Taking the total dust mass loss $\sim 3 \times 10^{16}$ g in the 1997 apparition of comet Hale-Bopp (Jewitt & Matthews 1999) as a representative dust supply rate (per comet per apparition), we estimate a cometary infalling rate of $\sim 7 \text{yr}^{-1}$, roughly consistent with the estimation of $< 15 \text{yr}^{-1}$ derived by Dent et al. (1995) from the observed CO upper limit assuming sublimating comets as a CO replenishment source in the ϵ Eri disk.⁶

The grain-grain collision timescale is only ≈ 0.1 Myr for dust at $r_p = 55$ AU, significantly shorter than the PR timescale τ_{PR} . But it is unlikely for grain-grain collisions to effectively remove the dust from the disk; instead, their major role is to re-distribute the dust over different size bins through fragmentation. The partially cleared central cavity is most likely created by the accumulation of gas and grains into planetesimals, as supported by the non-detection of circumstellar gas in this disk (Dent et al. 1995, Liseau 1999); and by the fact that the PR drag alone is not sufficient to clear the dust out to large radii up to ~ 30 AU (Jura 1990, Greaves et al. 1998, Dent et al. 2000).

Dent et al. (2000) modeled the ϵ Eri SED in terms of *compact* grains, assuming the dust absorption efficiency to be $Q_{\text{abs}} = 1$ for $\lambda < 30 \mu\text{m}$ and $Q_{\text{abs}} = (\lambda/30 \mu\text{m})^{-0.8}$ for $\lambda \geq 30 \mu\text{m}$, and adopting a uniform surface density distribution [i.e. $\sigma(r) \equiv \text{constant}$] in the range of $50 \lesssim r \lesssim 80$ AU. Satisfactory fit to the observed SED was achievable. Using emissivities calculated from real dust

⁴ Closer to the star, the threshold grain size below which grains will be ejected *increases* since $\tau_{\text{PR}} \propto r^2$ (see Eq.22 in Li & Lunine 2003b).

⁵In contrast, the cold outer ring is more likely to be collisionally replenished, although the sublimation of cometary CO volatiles (with a sublimation temperature of ~ 20 K) occurring inside $r < 110$ AU does generate dust outflow. But dust outflow only becomes significant when comets are close to the star, say, at $r \lesssim 3$ AU where H_2O ice starts to sublimate.

⁶If we adopt the Halley dust loss rate $\sim 1 \times 10^{14}$ g per orbit (Lisse 2002), we would expect a comet infall rate ~ 300 times more frequent. This is much higher than what is observed (~ 20 – 30 comets per year) for the present solar system. But we note that the number of cometary bodies and the bombardment rate were much higher at the early stage of our solar system. The solar system zodiacal cloud has a mass loss rate of $\sim 5 \times 10^{-14} m_{\oplus} \text{yr}^{-1}$; Lisse (2002) argued that the short-period comets alone are enough to supply the dust. In the β Pictoris disk, the number of *observed* cometary bodies (crossing the line of sight) is ~ 300 – 400 per year (Beust & Morbidelli 1996); however, the actual number would be much higher since many objects do not cross the line of sight and are therefore not visible in spectroscopy.

mixtures, however, Sheret, Dent, & Wyatt (2003) found that compact grains are not able to fit the observed SED.

The model presented in this *Letter* is somewhat simplified in the sense that we have assumed a symmetrical morphology for the ϵ Eri disk. Asymmetries and discrete flux enhancements (“clumps” or “bright spots”) are actually seen in its 850 μm SCUBA images (Greaves et al. 1998). As suggested by Ozernoy et al. (2000) and Quillen & Thorndike (2002), these features may be caused by the capture of grains into the mean motion resonances with a planet of Jupiter-mass embedded in the disk. This simplification would not affect the general conclusions of this *Letter* since the IR emission is mainly determined by the general distribution of dust in the disk, that is, a narrow ring.

5. Conclusion

The porous dust model, previously developed for the extended wedge-like disk around the ~ 15 Myr-old MS star β Pictoris and the narrowly confined ring-like disks around the Herbig Ae/Be stars HR 4796A (~ 8 Myr old) and HD 141569A (~ 5 Myr old), is shown also applicable to the dust disk around the ~ 800 Myr-old MS star ϵ Eri, the oldest “Big-Four” Vega-excess star. Modeled as a ring peaking at ~ 55 AU from the star with a FWHM ~ 30 AU, analogous to the young solar system Kuiper Belt, the observed IR to submillimeter emission as well as the 850 μm flux density radial distribution of the ϵ Eri disk is closely reproduced by porous grains of $\sim 7.1 \times 10^{-3} m_{\oplus}$ mass consisting of $\sim 90\%$ vacuum in volume. Predictions are made for future SIRTf/MIPS imaging observations that will offer a useful test of the porous dust model.

We thank J.S. Greaves, E.K. Holmes, A. Lecavelier des Etangs, R. Malhotra, K.A. Misselt, C. Papovich, W.T. Reach, G. Schneider, Z. Sekanina, M.D. Silverstone, and the anonymous referee for helpful discussions and/or suggestions. A. Li thanks the University of Arizona for the “Arizona Prize Postdoctoral Fellowship in Theoretical Astrophysics”. This research was supported in part by a grant from the NASA origins research and analysis program. G.J. Bendo is a Guest User of Canadian Astronomy Data Centre, which is operated by the Dominion Astrophysical Observatory for the National Research Council of Canada’s Herzberg Institute of Astrophysics.

REFERENCES

- Backman, D.E., & Paresce, F. 1993, in *Protostars and Planets III*, ed. E.H. Levy & J.I. Lunine (Tucson: Univ. Arizona Press), 1253
- Bendo, G.J., et al. 2003, *AJ*, 125, 2361
- Beust, H., & Morbidelli, A. 1996, *Icarus*, 120, 358
- Blum, J., Schräpler, R., & Kozasa, T. 2003, in preparation

- Cameron, A.G.W., & Schneck, P.B. 1965, *Icarus*, 4, 396
- Chini, R., Krügel, E., & Kreysa, E. 1990, *A&A*, 227, L5
- Chini, R., Krügel, E., Shustov, B., Tutukov, A., & Kreysa, E. 1991, *A&A*, 252, 220
- Dent, W.R.F., Walker, H.J., Holland, W.S., & Greaves, J.S. 2000, *MNRAS*, 314, 702
- Dent, W.R.F., Greaves, J.S., Mannings, V., Coulson, I.M., & Walther, D.M. 1995, *MNRAS*, 277, L25
- Draine, B.T., & Lee, H.M. 1984, *ApJ*, 285, 89
- Gillett, F.C. 1986, in *Light on Dark Matter*, ed. F.P. Israel (Dordrecht: Reidel), 61
- Greaves, J.S., & Holland, W.S. 2000, in *ASP Conf. Ser. 219, Disks, Planetesimals, and Planets*, ed. F. Garzón, C. Eiroa, D. de Winter, & T.J. Mahoney (San Francisco: ASP), 296
- Greaves, J.S., et al. 1998, *ApJ*, 506, L133
- Greenberg, J.M., & Li, A. 1999, *Space Sci. Rev.*, 90, 149
- Hatzes, A., et al. 2000, *ApJ*, 544, L145
- Henry, G.W., Donahue, R.A., & Baliunas, S.L. 2002, *ApJ*, 577, L111
- Jewitt, D.C., & Matthews, H.E. 1999, *AJ*, 117, 1056
- Jura, M. 1990, *ApJ*, 365, 317
- Krügel, E. 2003, *Physics of Interstellar Dust* (Bristol: IoP)
- Kurucz, R.L. 1979, *ApJS*, 40, 1
- Lagrange, A.-M., Backman, D.E., & Artymowicz, P. 2000, in *Protostars and Planets IV*, ed. V. Mannings, A.P. Boss, & S.S. Russell (Tucson: Univ. Arizona Press), 639
- Li, A., & Greenberg, J.M. 1997, *A&A*, 323, 566
- Li, A., & Greenberg, J.M. 1998, *A&A*, 331, 291
- Li, A., & Lunine, J.I. 2003a, *ApJ*, 590, 368
- Li, A., & Lunine, J.I. 2003b, *ApJ*, 594, 987
- Liseau, R. 1999, *A&A*, 348, 133
- Lissauer, J.J. 1993, *ARA&A*, 31, 129
- Lisse, C.M. 2002, *Earth, Moon, & Planets*, 90, 497

Ozernoy, L.M., Gorkavyi, N.N., Mather, J.C., & Taidakova, T.A. 2000, ApJ, 537, L147

Quillen, A.C., & Thorndike, S. 2002, ApJ, 578, L149

Sheret, I., Dent, W.R.F., & Wyatt, M.C. 2003, MNRAS, in press

Soderblom, D.R., & Däppen, W. 1989, ApJ, 342, 945

Weintraub, D.A., & Stern, S.A. 1994, AJ, 108, 701

Zuckerman, B. 2001, ARA&A, 39, 549

Zuckerman, B., & Becklin, E.E. 1993, ApJ, 414, 793

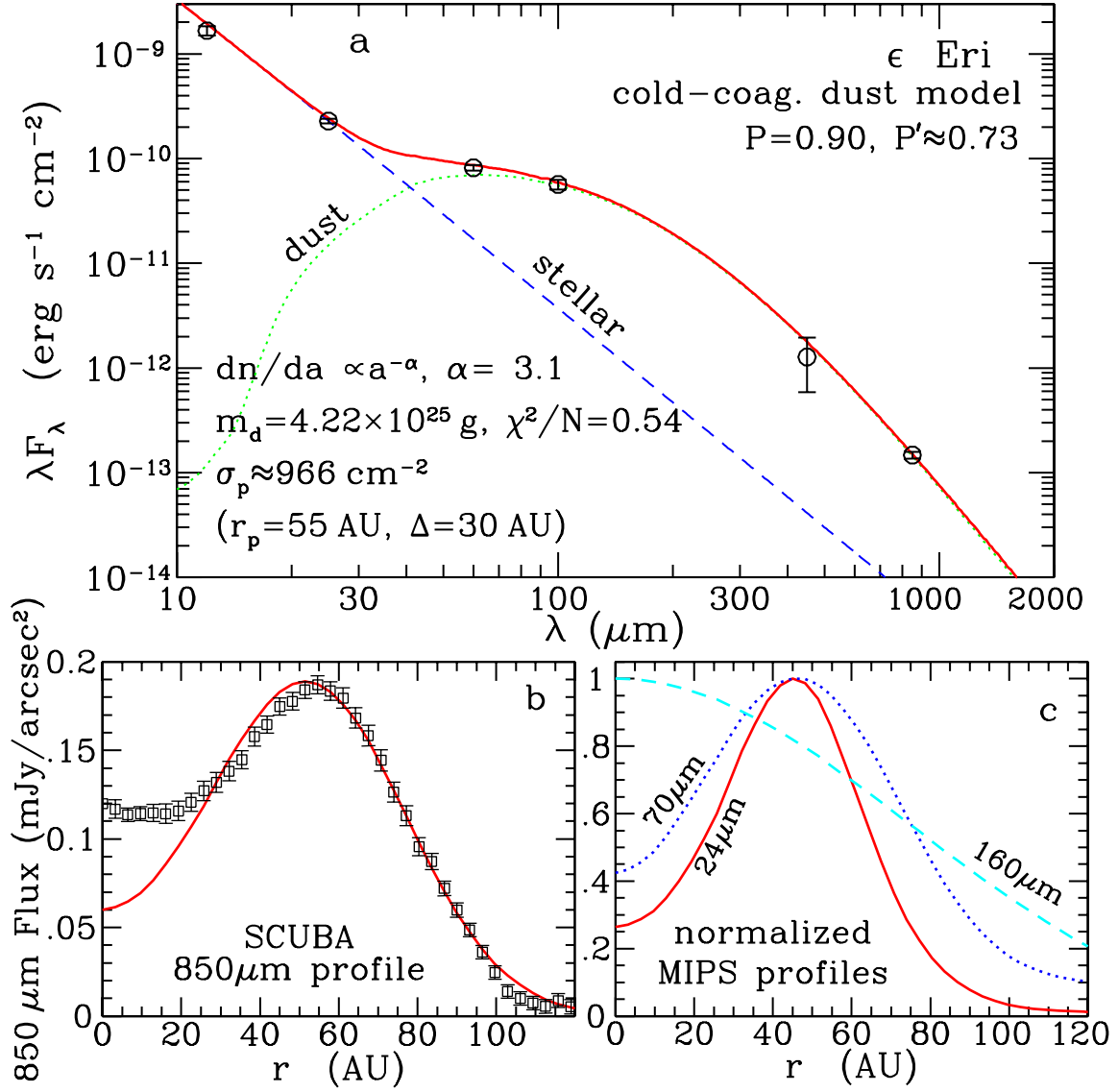


Fig. 1.— (a) IR to submillimeter emission of the ϵ Eri system (open circles: the 12, 25, 60, and 100 μ m IRAS data and the 450 and 850 μ m SCUBA data) compared with the model spectrum (solid line; which is the sum of the stellar [dashed line] and the dust [dotted line] contributions). (b) Radial profile of the dust emission at 850 μ m. Open squares plot the azimuthally averaged flux density radial distribution calculated from the SCUBA 850 μ m image (also see Figs. 1, 2 of Greaves et al. 1998 but theirs were smoothed with an 8'' Gaussian). The apparent rise within $r \approx 15$ AU is very likely artificial (see §3). Solid line plots the model-predicted 850 μ m emission radial profile convolved with the SCUBA 14'' beam. (c) Radial profiles predicted for the SIRTf MIPS bands at 24 μ m (solid line), 70 μ m (dotted line), and 160 μ m (dashed line). All profiles are convolved with the MIPS model PSFs and normalized to their peak values: ≈ 0.71 , 6.47, and 6.12 mJy arcsec $^{-2}$ for the 24, 70, and 160 μ m bands, respectively.

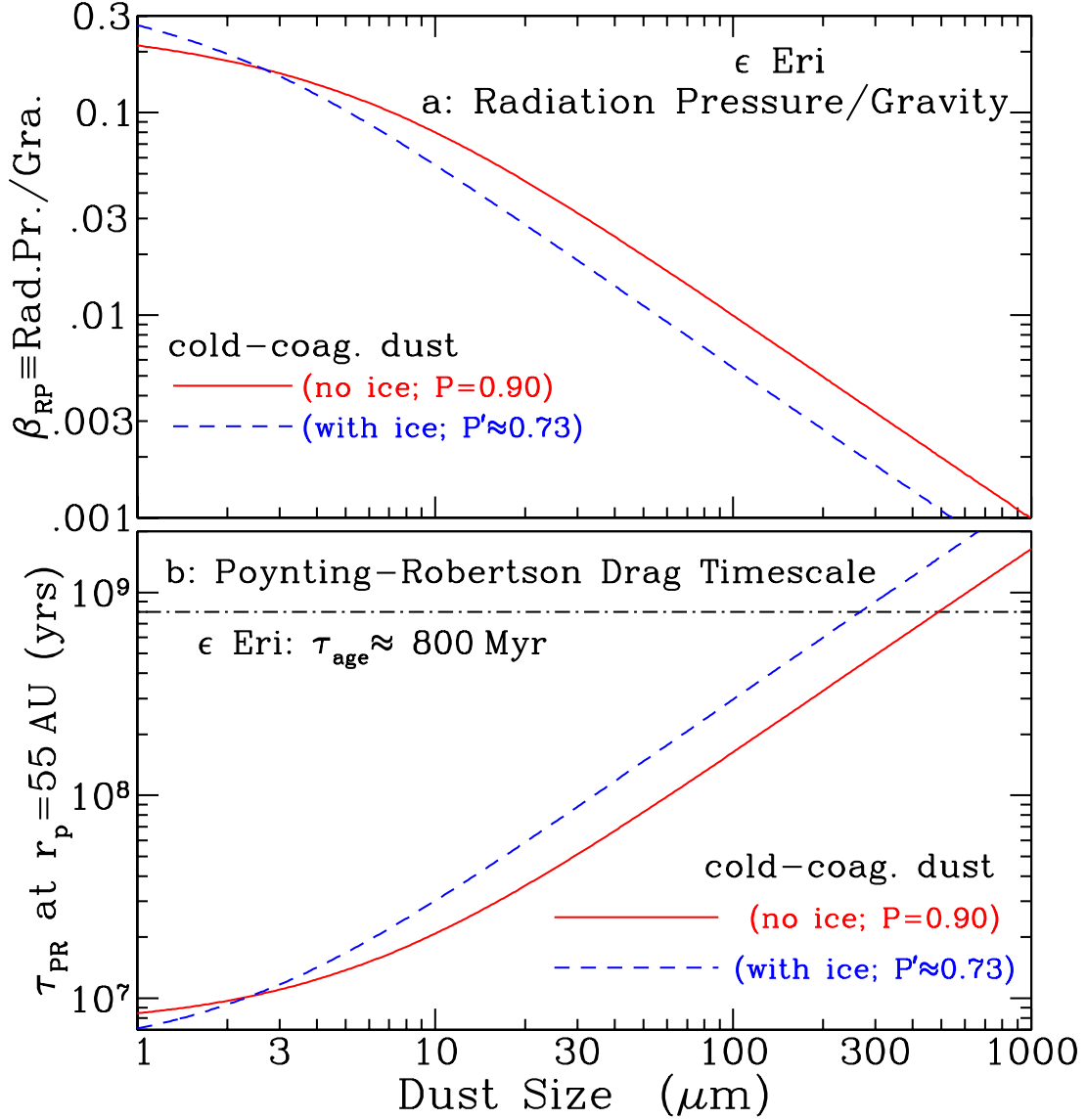


Fig. 2.— (a) Ratio of the radiative repulsion to the gravitational attraction (β_{RP}) for the best-fit “cold-coagulation” dust (without ice $P = 0.90$ [solid line] or with ice $P' = 0.73$ [dashed line]). (b) The orbit decay timescales τ_{PR} due to the Poynting-Robertson drag for the best-fit “cold-coagulation” dust (without ice $P = 0.90$ [solid line] or with ice $P' = 0.73$ [dashed line]) at a radial distance of $r_p = 55 \text{ AU}$ from the central star (note $\tau_{\text{PR}} \propto r^2$: the PR timescale decreases for dust at a smaller radial distance). The dot-dashed horizontal line plots the $\epsilon \text{ Eri}$ age ($\approx 800 \text{ Myr}$).